Modeling transcriptional feedback loops: The role of Gro/TLE1 in Hes1 oscillations

By Samuel Bernard[1], Branka Čajavec[1], Laurent Pujo-Menjouet[2], Michael C. Mackey[3*] and Hanspeter Herzel[1]

[1]*Institute for Theoretical Biology, Humboldt University, Invalidenstr. 43, 10115 Berlin, Germany.,* [2]*Vanderbilt University Department of Mathematics , 1326 Stevenson Center, Nashville, TN 37240, USA.,* [3]*Departments of Physiology, Physics & Mathematics and Centre for Nonlinear Dynamics, McGill University, 3655 Promenade Sir William Osler, Montreal, Qc, Canada, H3G 1Y6.*

[*]*Corresponding author, M.C. Mackey. Tel: (514) 398 4336, Fax: (514) 398 7452.*
mackey@cnd.mcgill.ca

The transcriptional repressor Hes1, a basic helix-loop-helix family protein, periodically changes its expression in the presomitic mesoderm. Its periodic pattern of expression is retained in a number of cultured murine cell lines. In this paper we introduce an extended mathematical model for Hes1 oscillatory expression that includes regulation of Hes1 transcription by Drosophila Groucho (Gro) or its vertebrate counterpart, the transducine-like enhancer of split/Groucho-related gene product 1 (TLE1). Gro/TLE1 is a necessary corepressor required by a number of DNA-binding transcriptional repressors, including Hes1. Models of direct repression via Hes1 typically display an expression overshoot after transcription initiation which is not seen in the experimental data. However, numerical simulation and theoretical predictions of our model show that the cofactor Gro/TLE1 reduces the overshoot and is thus necessary for a rapid and finely tuned response of Hes1 to activation signals. Further, from detailed linear stability numerical bifurcation analysis and simulations, we conclude that the cooperativity coefficient (h) for Hes1 self-repression should be large (i.e., $h \geq 4$). Finally, we introduce the characteristic turnaround duration, and show that for our model the duration of the repression loop is between 40 min and 60 min.

Keywords: Hes-1, Gro/TLE1, Hill coefficient, transcriptional repression loop, turnaround duration

1. Introduction

Recent experiments on cultured mammalian cell lines have shown oscillatory dynamics in the expression of at least three transcriptional factors: Hes1, p53 and NF-κB (Hirata *et al.*, 2002; Lev Bar-Or *et al.*, 2000; Hoffmann *et al.*, 2002; Lahav *et al.*, 2004). In this paper we deal with one of them, Hes1. We propose an extended model for the regulation of Hes1 expression that explains its oscillatory nature, and look for the common parameter requirements in another published model.

Somites are transient embryonic structures that are formed through segmentation of the presomitic mesoderm (PSM) in a highly regulated process called somitogenesis. They are the origin of the skeletal muscles of the body as well as the axial

skeleton and the dermis of the back (Christ & Ordahl, 1995; Gossler & Hrabe de Angelis, 1998). Two molecular systems operate during segmentation. The first one, called Notch signalling, plays an important role for the synchronization of adjacent cells through the Notch ligand Delta (forming the Delta/Notch complex) and for the precise positioning of the segment borders (Jouve *et al.*, 2000). It has been proposed that the Delta/Notch cell-cell signaling pathway sets up cell type boundaries by modulating cell fate according to the environmental cues (Heitzler & Simpson, 1991). Once stimulated, this complex induces the second molecular system, the segmentation "clock". It is an oscillatory mechanism generating periodic waves of gene expression. The period of these oscillations are short (order of 2 hours). This gene expression rhythm is called ultradian and can be described as follows.

Once the second molecular system is stimulated, the target genes are expressed. These genes produce a family of proteins called HES (for Hairy Enhancer of Split) (Gao *et al.*, 2001). The HES family of proteins are basic helix-loop-helix (bHLH) type transcriptional repressors. They are primary targets of Notch signaling and act by negatively regulating transcription of tissue-specific transcription factors (Ohsako *et al.*, 1994). The mammalian homolog of the 'hairy' gene in Drosophila, Hes1, has been found to be essential to neurogenesis, myogenesis, hematopoiesis, and sex determination (Proush *et al.*, 1994; Ishibashi *et al.*, 1995). Hes1 is a protein with a very short half-life of ≈30min. It is also known that a single serum treatment induces an oscillation of Hes1 mRNA and protein concentrations with a 2-hour period in a variety of cultured cells, such as myoblasts, fibroblasts, neuroblastoma cells and teratocarcinoma (Hirata *et al.*, 2002).

These oscillations are of particular relevance for somite formation in early development (Schnell & Maini, 2000; Bessho & Kageyama, 2003). The partitioning of the vertebrate body into a repetitive series of somites requires the spatially and temporally co-ordinated behaviour of cells in PSM. Hirata *et al.* (2002) also showed that Hes1 acts as its own repressor through a negative feedback loop. To account for the appearance of these oscillations, they proposed the involvement of a third factor in addition to Hes1 protein and Hes1 mRNA, because three species are necessary to induce oscillations in a negative feedback system (Griffith, 1968). However, the introduction of an explicit delay of 15–20 min in a basic two-species model with negative feedback is also sufficient to explain the oscillations (Jensen *et al.*, 2003; Monk, 2003). The delay accounts for the time needed for transcription, translation, and formation of a complex in the nucleus to start repression.

Drosophila Groucho (Gro) and its vertebrate counterparts, the transducine-like enhancer of split/Groucho-related gene products 1 to 4 (TLEs1 to 4), lack DNA binding ability but can functionally associate with a number of DNA-binding proteins, including Hes1. Interaction with Gro/TLE1 at the nuclear matrix is necessary for transcriptional repression by Hes1 (McLarren *et al.*, 2001). Hes1 itself activates hyperphosporylation of Gro/TLEs bound to it. This correlates with association with a nuclear matrix, suggesting that chromatin remodeling might be a mechanism for this transcriptional repression (Nuthall *et al.*, 2002). Therefore, we present here a model that includes Gro/TLE1 in the regulation of Hes1 mediated repression of transcription.

It is well known that systems of ordinary differential equations (ODEs) with negative feedback loops need to be at least three-dimensional to sustain oscillations. A requirement for these oscillations is a high cooperativity coefficient, i.e. a large

feedback gain is necessary for the onset of oscillations (Tyson & Othmer, 1978). One such system, the Goodwin model (Goodwin, 1965), has been extensively used in circadian clock modeling. However, this model requires a cooperativity coefficient of at least 9 to induce oscillations which is large and unrealistic unless a cascade mechanism is involved (Ferrell, 1996). On the other hand, the introduction of a time delay in a feedback loop allows sustained oscillations even in a one-dimensional delay differential equation with a relatively low cooperativity coefficient. Negatively regulated systems with delays have been used in various biological contexts, from haematopoietic (blood cell production) diseases to pupil light reflex (Beuter *et al.*, 2003). In these examples, the relevance of delays is uncontested and their usage has been of an appreciable utility in explaining nonlinear phenomena. Small gene regulation systems have also been the object of recent mathematical modeling (Santillan & Mackey, 2004*a*,*b*).

With the Hes1 data and system as a guide, this paper considers two different models of self-repression kinetics, and uncovers conserved features among them. Section 2 presents an analysis of the two-dimensional system proposed by Jensen *et al.* (2003). In §3 we develop an extension of the Jensen et al. model considering Gro/TLE1 interaction with the Hes1 regulatory pathway. We then discuss the effects of Gro/TLE1 on the properties of oscillatory Hes1 expression after initiation by a serum shock. Section 4 considers general features of the two models that allow the estimation of parameter values. We find quantities that are relatively invariant with respect to different models. We conclude that although interaction of Hes1 with the corepressor Gro/TLE1 is not necessary for oscillatory expression of Hes1, it does allow a much more realistic activation curve that is consistent with the experimental data.

2. Two-dimensional Hes1–mRNA repression model

Standard mathematical analysis shows that two-component models with a negative feedback can not have stable self-sustained oscillations. Two possibilities are then offered for a simple extension of the model to achieve oscillatory behavior.

In the first, one can invoke the existence of a third dependent variable. This is the route taken by Hirata *et al.* (2002) who have considered a three-dimensional system, in which a third (unknown) species X actively degrades Hes1, while Hes1 also acts as a repressor for X. However, the analysis of this model is not further considered in this paper. In the second possibility, an explicit delay (Jensen *et al.*, 2003; Monk, 2003; Lewis, 2003) is considered, which has its origin in the underlying biology. In either case the Hill coefficient h, which accounts for the cooperativity of repression activity of agents involved in the inhibition of Hes1 transcription, is crucial. Although these studies dealt with parameter estimation and stability analysis, the cooperativity coefficient h was taken as a fixed parameter with a value between 2 and 4. Takebayashi *et al.* (1994) showed that Hes1 regulatory region has four N box sequences and that Hes1 binds to these sequences. Furthermore when the N box sequences are disrupted, repression activity of Hes1 is severely impaired. The complexity of transcription regulation does not allow for direct evaluation of the cooperativity coefficient and thus, the results presented in this section are used to set plausible ranges on the value of h.

Table 1. *Parameter list*

(Parameters used for simulations and analysis. The "m" indicates that the parameter was estimated from model analysis. References are: 1= (Hirata *et al.*, 2002); 2= (Jensen *et al.*, 2003; Monk, 2003) and 3= (Bolouri & Davidson, 2003).)

Parameter	Value	Units	Ref.	Description
α	0.031	min^{-1}	(1)	Hes1 degradation rate.
δ	0.029	min^{-1}	(1)	mRNA degradation rate.
σ	0.030	min^{-1}	m	GroH deactivation rate.
k	—	au	(2)	See Appendix A.
h	$2 \sim 4$	—	(2),m	Hes1 repression cooperativity. Lower bound.
u	$2 \sim 4$	—	m	GroH activation cooperativity. Lower bound.
T_{Hopf}	$90 \sim 150$	min	(1)	Period of oscillation of Hes1.
τ	$10 \sim 40$	min	(2),m	Total delay due to transcription, translation and transport. Upper bound.
f_0	1	min^{-1}	(3)	Maximal transcription/translation rate. See Appendix A.
g_0	1	min^{-1}	—	Maximal phosphorylation rate.
β	1	min^{-1}	(3)	Hes1 translation rate.

A two-compartment model for Hes1–mRNA self-repression with delay can be written as (Jensen *et al.*, 2003; Monk, 2003; Lewis, 2003),

$$\frac{\mathrm{d}mRNA(t)}{\mathrm{d}t} = \frac{f_0 k^h}{k^h + Hes1(t-\tau)^h} - \delta\, mRNA(t), \tag{2.1}$$

$$\frac{\mathrm{d}Hes1(t)}{\mathrm{d}t} = \beta\, mRNA(t) - \alpha\, Hes1(t). \tag{2.2}$$

Equations (2.1), (2.2) will be referred to as Model A. The first equation describes the cellular concentration of Hes1 mRNA (*mRNA*) at time t and the second equation describes the cellular concentration of Hes1 protein (*Hes1*) at time t. The respective degradation rates (δ of *Hes1* and α of *mRNA*) and translation rate (β) all have units of min^{-1}. The nonlinearity comes from the transcriptional repression activity of Hes1. The parameters in the feedback loop are the maximum mRNA transcription rate f_0 (min^{-1}), a DNA dissociation constant k (same units as *Hes1*) and a Hill coefficient h representing the degree of cooperativity between different factors intervening in the repression of Hes1 gene by Hes1 protein. The delay τ accounts for the delay due to Hes1 modification, complex formation and nucleocytoplasmic molecular transport.

Table 1 gives the values of parameters used for the analysis and simulations. The details of the computations and analysis are given in Appendix A a.

In this model, a linear stability analysis (cf. Appendix A a) leads to analytical formulae for local stability connecting the Hill coefficient, Hopf (oscillation) period and rate constants. Namely, the steady state is locally unstable whenever h is larger than,

$$h_A \equiv \left[\left(\frac{4\pi^2}{\alpha\delta T_{Hopf}^2} + \frac{\delta}{\alpha} \right) \left(\frac{4\pi^2}{\alpha\delta T_{Hopf}^2} + \frac{\alpha}{\delta} \right) \right]^{1/2}. \tag{2.3}$$

Assuming a period $T_{Hopf} = 120$ min, we obtain a lower bound on the cooperativity coefficient h_A of $h_A \simeq 4.1$. The associated critical delay τ_{crit}^A can be expressed as,

$$\tau_{crit}^A \equiv \arccos\left(\frac{\omega^2}{\alpha\delta h} - \frac{1}{h} \right) \times \omega^{-1}, \tag{2.4}$$

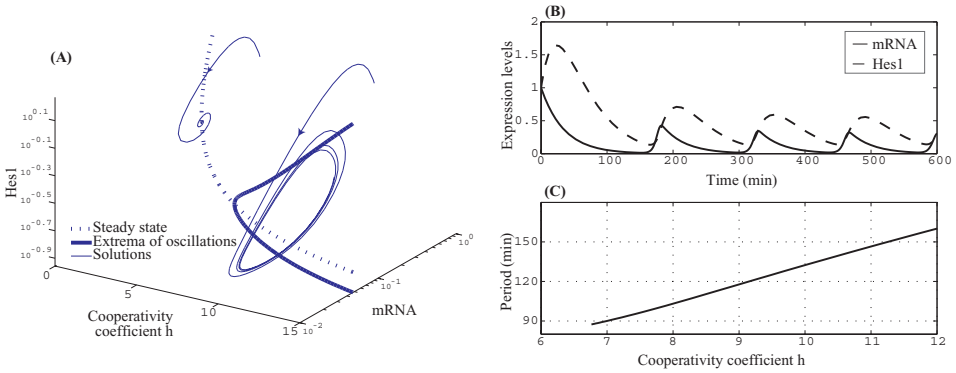

Figure 1. (*A*) Numerically computed bifurcation diagram of Model A as a function of the cooperativity coefficient h. The Hopf bifurcation occurs at the intersection of the thick and dotted lines. The Hill coefficient has an influence on the amplitude of the Hes1 oscillation. The thick solid lines represent the maxima and minima of the periodic solutions, whereas the dotted curve represents the steady-state Hes1 and mRNA levels. The thin lines show two solutions for values of h below and above the bifurcation point. For $h = 3$, there is a spiral convergence to a steady state. For $h = 10$, the solution converges to a stable limit cycle. (*B*) Time evolution of the limit cycle illustrated in panel (*A*). (*C*) Period of oscillation of the limit cycle as a function of h. In all panels, the parameters are as in table 1, except $\tau = 11$ min.

where ω is the oscillatory angular frequency, $\omega = 2\pi/T_{Hopf}$. This leads to a value of the maximal τ^A_{crit}, $\tau_A \simeq 19.7$ min. (Refer to Appendix A a for a complete analysis.)

When Model A has no explicit delay ($\tau = 0$), its characteristic time scale (CTS), defined as the inverse of the absolute value of the real part of the eigenvalue λ (cf. Appendix B), is determined by the decay rates α and δ (Murray, 1993; Strogatz, 1994). Explicitly, CTS $= 2\,(\alpha + \delta)^{-1} = 33.3$ min. Added to $\tau_A = 19.7$ min, it gives a characteristic turnaround duration (CTD) of CTD = CTS $+\tau_A = 53$ min. The turnaround duration is the time required to have an effective repression after transcription initiation (see Appendix B for a derivation of these results). As noted in the Introduction, other proteins with short half-lives are known to have oscillatory behavior as well, such as p53 and NF-κB.

The value τ_A constitutes an upper bound on the delay and h_A is a lower bound on the cooperativity coefficient. To have large amplitude oscillations (that is, to move away from the bifurcation point), it is necessary to have a somewhat smaller τ and/or larger h. In figure 1, the delay τ was fixed at 11 min, and the bifurcation diagram is plotted for varying h. The oscillations and the associated period are shown in the two right hand panels.

3. Gro/TLE1–mediated repression allows tuned response

(*a*) *Gro/TLE1–Hes1 repression model*

We now consider the influence of an additional factor known to be involved in the Hes1 repression loop, namely Gro/TLE1. Protein Gro/TLE1 is activated through Hes1-induced hyper-phosphorylation. This activation is described by a monotonically increasing Hill function with Hill coefficient u. Moreover, the active form

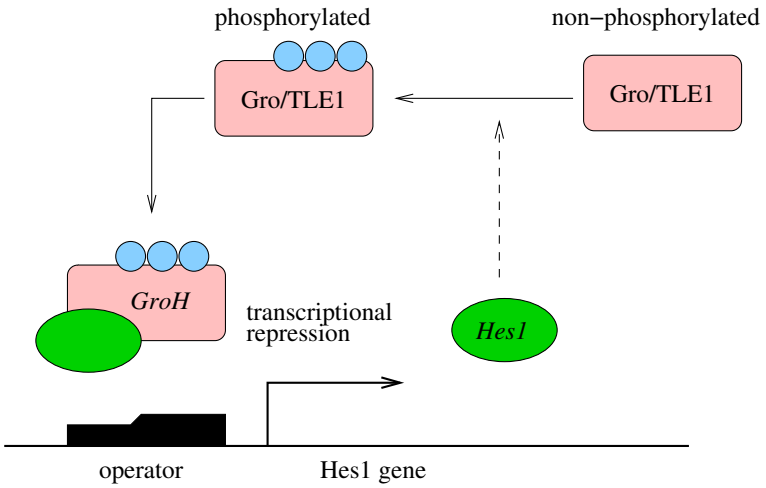

Figure 2. Model for Gro/TLE1-mediated Hes1 repression.

of Gro/TLE1 forms a complex with Hes1, denoted $GroH$, to mediate repression through a negative feedback loop (cf. figure 2). The variable $GroH$ represents the repression complex of hyper-phosphorylated Gro/TLE1 with Hes1 protein. The associated equations are written as

$$\frac{\mathrm{d}Hes1(t)}{\mathrm{d}t} = \frac{f_0 k^h}{k^h + GroH(t-\tau)^h} - \alpha Hes1(t), \tag{3.1}$$

and

$$\frac{\mathrm{d}GroH(t)}{\mathrm{d}t} = \frac{g_0 Hes1(t)^u}{\ell^u + Hes1(t)^u} - \sigma GroH(t). \tag{3.2}$$

These equations constitute what we call Model B. As with the other two models, local stability considerations establish relationships between the Hill coefficient, period, kinetic constants and delay for Model B (cf. Appendix A b). Denoting the total cooperativity coefficient by $c = uh$, we obtain an expression similar to equation (2.3):

$$c = \left[\left(\frac{4\pi^2}{\alpha\sigma T_{Hopf}^2} + \frac{\sigma}{\alpha}\right)\left(\frac{4\pi^2}{\alpha\sigma T_{Hopf}^2} + \frac{\alpha}{\sigma}\right)\right]^{1/2}. \tag{3.3}$$

Again, we can calculate the critical delay τ_{crit}^B,

$$\tau_{crit}^B = \arccos\left(\frac{\omega^2}{\alpha\sigma c} - \frac{1}{c}\right) \times \omega^{-1}. \tag{3.4}$$

The introduction of another nonlinearity does not change the linear stability analysis performed for Model A. It should be noted, however, that this analysis is an approximation and more detailed numerical analysis shows that the Hill coefficient threshold h_A is slightly higher than predicted (2.5 instead of 2.0 for fixed $u = 2.0$). The characteristic turnaround duration has, as for Model A, a value of CTD = 53 min.

Figure 3 (bottom) shows the stability boundary in (h, τ) space for Models A and B, while the top part of the figure gives the corresponding Hopf period. The region

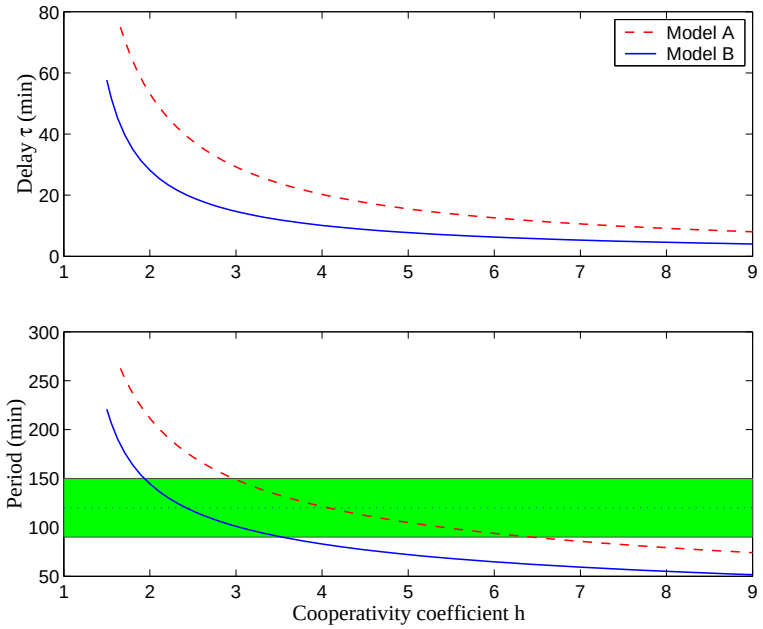

Figure 3. Comparison between numerical bifurcation analysis of Model A (*dashed lines*) and Model B (*solid lines*). Notice that the small Hill coefficient needed in case of Model B comes from the fact that the total cooperativity coefficient is $h \times u$. (*A*), the bifurcation curves give the delay τ required to induce a Hopf bifurcation for a given h. Crossing the lines from left to right (or from below) due to parameter variation induces oscillations (see e.g. figure 1). (*B*), associated periods for each bifurcation curve are shown. The grey area indicates the period interval from 90 to 150 min leading to ranges of the corresponding Hill coefficients.

of oscillatory expression is above and to the right of the (h, τ) curves. For Model B, only the Hill coefficient h is shown. With $u = 2$, the total cooperativity coefficient is thus doubled, leading to almost the same result as for Model B. Thus, for a 120 min period oscillation, the corresponding values of h and τ can be uniquely determined. For Model B, the Hill coefficient required for 120 min period oscillations is greater than 2.5 and the delay smaller than $\max(\tau^B_{crit}) \equiv \tau_B = 20$ min. If an interval between 90 and 150 min for the period is considered, a range for h and τ can be defined:

– for Model A, $3 < h_A < 7$, and 15 min $< \tau_A <$ 30 min;

– for Model B, $4 < c < 8$, and 10 min $< \tau_B <$ 30 min.

These results show that introducing and new mechanisms does not affect the basic properties of these models with respect to the Hopf bifurcation. Interestingly, the model considered by Hirata *et al.* (2002) consists of three ODEs with two feedback loops, each with a Hill coefficient of 2 giving a total cooperativity coefficient of 4. Our comparison of these models reveals general properties of the Hes1 oscillation that are not yet measured experimentally. In particular, strong cooperativity of Hes1 repression (h between 3 and 8) and a turnaround duration between 40 min and 60 min are predicted.

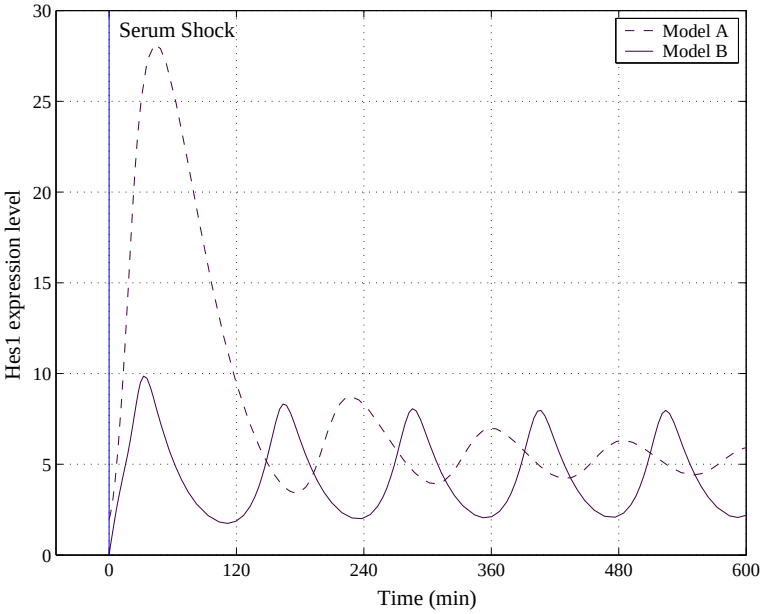

Figure 4. Introduction of a second nonlinearity allows Hes1 expression to rapidly approach a steady oscillation after initiation by serum shock (*solid line*), compared with the behavior of Model A (*dashed line*).

(*b*) *A second nonlinearity to increase adaptativity*

The stability results of the previous sections show that oscillation onset of the systems depends on model independent quantities such as degradation rates, cooperativity coefficients (or the product thereof), and the characteristic turnaround duration, including delays due to auxiliary variables. The CTD takes into account both the time scale introduced by the dynamics of the non-delayed system and the explicit delay τ. However, the behavior of the solution away from the steady state can be quite different from model to model.

Experimental data on Hes1 expression level in cultured cells after a serum shock shows no sign of overshoot in the first cycle of mRNA transcription and Hes1 synthesis (Hirata *et al.*, 2002). On the contrary, the expression levels of both mRNA and Hes1 rapidly settle down to an oscillatory regime of approximately constant amplitude. Systems with only one nonlinearity often display a large overshoot before solutions converge to their attractor. A second nonlinearity is then needed to fine tune the dynamics of the systems when away from equilibrium. In Appendix C, using Model A, we compute a lower bound for the value of the Hes1 expression overshoot with respect to the steady-state value.

From the results of a full numerical simulation of Models A and B, figure 4 compares the initiation of Hes1 synthesis after a serum shock. The serum shock triggers Hes1 transcription and is modelled by setting *Hes1*, *mRNA* and *GroH* initial levels to values close to zero at time 0. In Model A, there is an overshoot due to the lack of repression mechanisms in the first minutes. In the case of Gro/TLE1-mediated repression (Model B), it is assumed that Gro/TLE1 is already active at a

low level, and the fast activation rate of Gro/TLE1 supports the rapid convergence of Hes1 expression to the stable oscillatory pattern.

Even though Model A consists of a nonlinear system with a delayed variable, it can be solved analytically for a short time given certain initial conditions. It is thus possible to give a formal bound for the overshoot. The following calculation shows that the large overshoot displayed in figure 4 is a characteristic feature of Model A.

We assume that before initiation the Hes1 gene is practically silent so the initial conditions for *mRNA* and *Hes1* are set to zero. Moreover, to simplify the computations, we set $\alpha = \delta$. From table 1 one can see that this is a reasonable assumption. To obtain a simple expression for the overshoot, we set the transcriptional delay τ equal to the half-lives of Hes1 mRNA and protein, so $\tau = \ln 2/\delta \simeq 23$ min. Calculations given in Appendix C lead to a bound of the overshoot in Hes1 expression of $Hes1_{overshoot} \geq (1 - \ln 2)\beta f_0/(2\delta^2)$. With a steady state of $Hes1_* = \beta/\alpha$ the ratio between the maximal expression level and the steady-state level is

$$\frac{Hes1_{overshoot}}{Hes1_*} = (1 - \ln 2)\frac{f_0}{\delta}. \tag{3.5}$$

From table 1, the ratio of maximal transcription to degradation rates, f_0/δ, is large. For instance, f_0/δ to 30, gives an overshoot about ten times the steady-state value. It is likely that the ratio f_0/δ is even higher since estimates of 11 initiations per second have been reported (Bolouri & Davidson, 2003). It is possible to reduce the overshoot considerably by setting some parameters to unrealistic values. For example, a translation rate β of one translation every 33 min (0.03 min^{-1}) leads to a smaller overshoot, comparable to Model B simulations. It is likely, however, that β is much larger, ranging from 1.0 min^{-1} to 100 min^{-1} (Ghaemmaghami *et al.*, 2003; Bolouri & Davidson, 2003). Even though β has no effect on the stability properties of these models, it is initially of crucial importance after serum shock.

In principle one could replace β in Model A by a nonlinear function without having to take Gro/TLE1–Hes1 interactions into consideration. However, even though this is biologically plausible, the introduction of this nonlinearity is not motivated by any experimental data and would be artificial.

Compared to Model A, Model B shows a more realistic activation curve. This is due to two factors. First, since Gro/TLE1 is a general corepressor, there may exist a baseline level of phosphorylated protein in the cell before initiation of Hes1 synthesis. This will have an attenuating effect on Hes1 transcription. Second, numerical simulations show that in Model B a smaller delay τ is needed to generate 120 min period oscillations due to the introduction of a second nonlinearity. Consequently, the speed of the response after activation is increased.

4. Discussion

Numerical simulations and analytical results from three models of Hes1 self-regulation show interesting model-independent features. Encouragingly, the most important characteristics of the models all lie in the same range. Thus, to be consistent with the experimental data the cooperativity coefficient associated with Hes1 repression must be higher than 2, and is likely to be on the order of 4. Further, the explicit delay included in the model must be of the order of tens of minutes, ranging from 10 min to 50 min depending on the model. The characteristic turnaround duration

(CTD), however, is less variable. In all model versions, a CTD of about 40 to 60 min is predicted. An explicit delay $\tau < 20$ min seems to be particularly well suited for two-component regulatory loops. These results are in agreement with previous studies (Hirata *et al.*, 2002; Jensen *et al.*, 2003; Monk, 2003; Lewis, 2003). Moreover, we have estimated here the value of the cooperativity coefficient, making the mathematical analysis more complete. Given the complex nature of transcription regulation, it is likely that this parameter plays an important role in the control of protein expression.

A linear stability analysis allows one to make estimates of cooperativity coefficients and delays from measured kinetic data, such as Hes1 protein and mRNA degradation rates and the period of oscillation. The linear analysis also makes it possible to derive a lower bound for the cooperativity coefficient h and an upper bound for the delay τ. It is, however, difficult to evaluate the converse: i.e., a lower bound for τ and an upper bound for h. However, under the assumption that the system is not too far away from the Hopf bifurcation, the range of periods seen in different experiments allows us to estimate the range of h and τ. Thus, when periods are between 90 and 150 min, the total cooperativity coefficient should range between 3 and 8, with a corresponding delay between 10 and 30 min.

A central quantity introduced in this study is the characteristic turnaround duration (CTD), defined as the characteristic time between transcription initiation and repression. The CTD is derived from the linear analysis and should be regarded as an upper bound. The model-independent estimation of CTD $\simeq$ 50 min is a central result based only on partial knowledge of kinetic data. The use of different models is justified as long as model-independent characteristics of Hes1 dynamics are conserved. These results are likely to be similar in other negative transcriptional feedback loops involving, for example, p53, NF-κB or circadian clock genes.

Interaction of Hes1 with Gro/TLE1 is necessary for transcriptional repression by Hes1 (McLarren *et al.*, 2001). The fact that Hes1 itself activates hyperphosphorylation of Gro/TLEs bound to it suggests a dynamic link between the two proteins. Introduction of Gro/TLE-mediated repression in a model allows a faster physiological adaptation after a serum shock and/or Hes1 induction from the Notch pathway. In feedback loop systems with a single nonlinearity, a large overshoot is seen after initiation, resulting in an initial strong response followed by smaller oscillations. When the corepressor Gro/TLE1 is introduced, the overshoot is greatly reduced, and steady oscillatory protein expression levels are observed. Gro/TLE1 is known to be expressed in a variety of cell lines and acts as a general corepressor (Jimenez *et al.*, 1997). We suggest that the kinetic role of Gro/TLE1 is to fine tune expression levels after initiation of protein synthesis.

This work was supported by MITACS (Canada) and the Natural Sciences and Engineering Research Council (NSERC grant OGP-0036920, Canada). We especially thank Drs. M. Santillán, S. Stifani and R. Kageyama for helpful discussions and comments. This work was initiated while BČ was visiting the Center for Nonlinear Dynamics, McGill University. We acknowledge support from the German grant agencies BMBF and DFG.

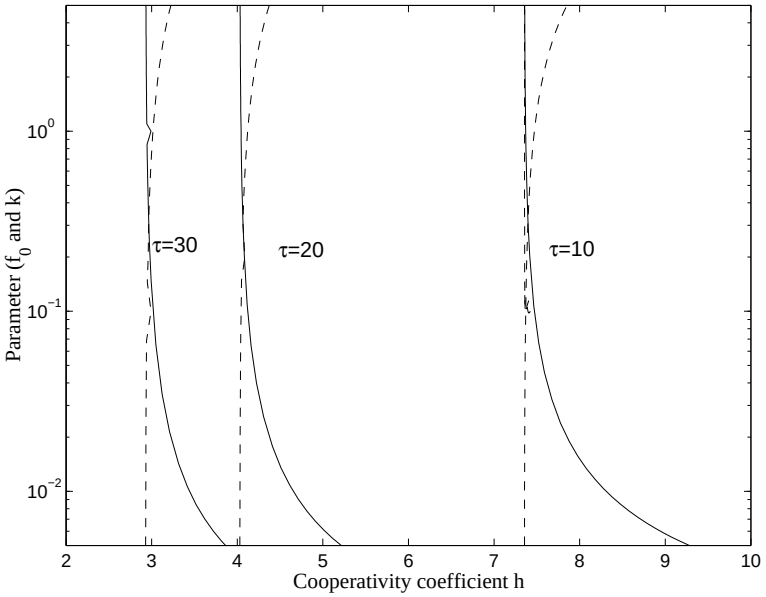

Figure 5. Robustness of the bifurcation parameter h with respect to parameters f_0 (*solid lines*) and k (*dashed lines*). Different curves are shown for different values of the delay ($\tau = 10$, 20 and 30 min). Each curve represent the value of either parameter (f_0 or k) at which a Hopf bifurcation occurs when the parameter h is varied. The stability region lies on the left-hand-side of the curves.

Appendix A. Linear stability analysis

(*a*) *Model A*

In this section, we present a detailed linear stability analysis for Model A. The linear analysis for Model B follows the same scheme, and is outlined below in the next section.

Equations (2.1, 2.2) are nonlinear differential equations with a delayed negative feedback. [For a general introduction to delay differential equations and their applications, see Hale & Verduyn-Lunel (1993) and Beuter *et al.* (2003).] The first step of the linear stability analysis is the calculation of the steady states. The equations defining the steady-state are

$$\delta\, mRNA_* = \frac{f_0 k^h}{k^h + Hes1_*^h}, \tag{A 1}$$

and

$$\alpha\, Hes1_* = \beta\, mRNA_*. \tag{A 2}$$

We note that f_0 and k have only a minor effect on the bifurcation analysis. Figure 5 shows that even changes of one order of magnitude do not substantially affect the bifurcation analysis. For example, a change of k from 0.01 to 1 leads to a change of the bifurcation parameter h from 4.0 to 4.1, at a delay of $\tau = 20$ min. As long as k takes small values, the parameter k can be freely chosen without perturbing the

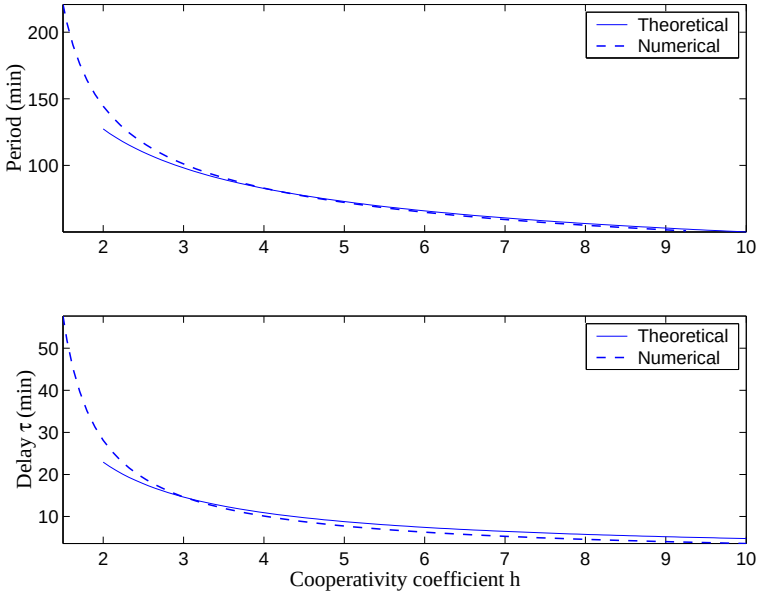

Figure 6. Comparison between theoretical and numerical bifurcation analysis of Model B. (*A*) The numerically computed bifurcation curve (*dashed-dotted line*) shows the value τ at which a Hopf bifurcation occurs when h is varied. The theoretical bifurcation curve (*solid line*) was drawn using Eq. 3.4). Note the good agreement between the numerical and theoretical curves for larger h. (*B*) The corresponding period of oscillation (T_{Hopf}) is shown. The numerically computed period (*dashed-dotted line*) is compared to the theoretically computed period (*solid line*) using $T_{Hopf} = 2\pi/\omega$ with ω defined in Eq. A 18.

bifurcation analysis of Model A. An appropriate scaling is

$$\left(\frac{k\alpha}{\beta}\right)^h = \frac{\delta}{f_0 - \delta}. \tag{A 3}$$

With this scaling, the steady-state values are $mRNA_* = 1$ and $Hes1_* = \beta/\alpha$. This is a reasonable assumption since $f_0 \gg \delta$ (see table 1), at least for larger h, as shown in figure 6. Figure 6 shows the comparison between results using the choice of k discussed above and bifurcation analysis performed with the `MATLAB` package `DDE-BIFTOOL` (Engelborghs *et al.*, 2001). There is an excellent agreement between the analytical approximation and numerical results.

Linearization of equations (2.1, 2.2) around this steady state yields the following equations for the deviations from the steady states $x = mRNA - 1$ and $y = Hes1 - \beta/\alpha$:

$$\frac{\mathrm{d}x}{\mathrm{d}t} = -\delta x + f'_* y_\tau, \tag{A 4}$$

$$\frac{\mathrm{d}y}{\mathrm{d}t} = \beta x - \alpha y. \tag{A 5}$$

Here f is the nonlinear function on the right hand side of equation (2.1) defined by,

$$f = f_0 \frac{k^h}{k^h + Hes1^h}. \tag{A 6}$$

Its derivative, evaluated at the steady state f'_*, is given by

$$f'_* = -\frac{\alpha\delta h}{\beta}\left(1 - \frac{\delta}{f_0}\right). \tag{A 7}$$

The characteristic (eigenvalue) equation associated with this system of equations is

$$(\lambda+\delta)(\lambda+\alpha) + \alpha\delta h\left(1 - \frac{\delta}{f_0}\right)\exp(-\lambda\tau) = 0. \tag{A 8}$$

At the Hopf bifurcation point, a pair of eigenvalues λ has a zero real part, that is, $\lambda = i\omega$. The value ω gives the frequency of oscillation at the Hopf bifurcation point. In model A, the frequency is given by,

$$\omega = \frac{1}{\sqrt{2}}\left[-(\delta^2+\alpha^2) + \left[(\delta^2-\alpha^2)^2 + 4\alpha^2\delta^2h^2\left(1-\frac{\delta}{f_0}\right)^2\right]^{1/2}\right]^{1/2}. \tag{A 9}$$

The assumption $f_0 \gg \delta$ allows us to simplify the expression for h_A (equation (2.3)), which is found by solving equation (A 9) with $\omega = 2\pi/T_{Hopf}$. The oscillation onset (Hopf bifurcation) is given by a sign change of the real part of λ in the characteristic equation for $\lambda = i\omega$. Then, by solving the characteristic equation of Model A (equation (A 8)) for τ, we find the relation given in equation (2.4).

(*b*) *Model B*

For Model B the steady-state equations are

$$\delta\, Hes1_* = \frac{f_0 k^h}{k^h + GroH_*^h}, \tag{A 10}$$

$$\alpha\, GroH_* = \frac{g_0 {Hes1}_*^u}{\ell^u + {Hes1}_*^u}. \tag{A 11}$$

Two scalings are possible, for k and ℓ, and we define, $k^h = \alpha/(f_0-\beta)$ and $\ell^u = \sigma/(g_0-\sigma)$. These scalings are valid when $f_0 \gg \alpha$ and $g_0 \gg \sigma$. The steady states will then be $Hes1_* = 1$ and $GroH_* = 1$. The linear approximation around the steady states for the deviations $x = Hes1 - 1$ and $y = GroH - 1$ leads to the following equations:

$$\frac{\mathrm{d}x}{\mathrm{d}t} = -\alpha x + f'_* y_\tau, \tag{A 12}$$

and

$$\frac{\mathrm{d}y}{\mathrm{d}t} = g'_* x - \sigma y, \tag{A 13}$$

wherein the derivatives of the nonlinearities at the steady states are

$$f'_* = -\alpha h\left(1 - \frac{\alpha}{f_0}\right), \tag{A 14}$$

and

$$g'_* = -\sigma u\left(1 - \frac{\sigma}{g_0}\right). \tag{A 15}$$

This ultimately leads to the eigenvalue equation

$$(\lambda+\alpha)(\lambda+\sigma)+\Gamma\exp(-\lambda\tau)=0, \tag{A 16}$$

in which

$$\Gamma=\alpha h\sigma u\left(1-\frac{\alpha}{f_0}\right)\left(1-\frac{\sigma}{g_0}\right). \tag{A 17}$$

At the Hopf bifurcation, $\lambda=i\omega$ gives

$$\omega=\frac{1}{\sqrt{2}}\left[-(\alpha^2+\sigma^2)+[(\alpha^2-\sigma^2)^2+4\Gamma^2]^{1/2}\right]^{1/2}. \tag{A 18}$$

Finally, by making the approximation that $\Gamma\simeq hu\alpha\sigma$, and solving equation (A 18) for hu, equation (3.3) and, subsequently, equation (3.4) are obtained.

Appendix B. Characteristic turnaround duration (CTD)

When $\tau=0$, Model A reduces to a system of ordinary differential equations (ODEs) with a stable steady state. The linearized equations of Model A become linear ODEs, and the eigenvalues λ are given by equation (A 8) with $\tau=0$. That is,

$$(\lambda+\delta)(\lambda+\alpha)+\alpha\delta h\left(1-\frac{\delta}{f_0}\right)=0. \tag{B 1}$$

Hence, $\lambda=[-(\alpha+\delta)\pm\sqrt{\Delta}]/2$, with a negative discriminant $\Delta<0$ when $\delta=\alpha$. Thus, the real part of λ is $-(\alpha+\delta)/2$. The turnaround time $|\lambda|^{-1}+\tau$ gives an estimation of the time required from mRNA synthesis to repression of transcription, i.e., a complete turn around.

Figure 7 shows the characteristic turnaround duration Models A and B as a function of the cooperativity coefficient (h for Model A and c for Model B). The CTD curves for Model A and B vary are very similar and vary very weakly. Thus, when h varies from 4 to 10, the CTD only decreases from 53 min to 44 min.

Appendix C. Overshoot and adaptativity

We discuss here the maximal value that solutions of Model A can achieve for initially vanishing Hes1 mRNA. Numerical simulations show that this maximal value is reached around $t=\tau$. This will restrict our search to the interval $t\in(0,\tau]$ leading to a lower bound of the maximal value of Hes1 concentration.

Since the non-delayed terms are linear, Model A can be solved directly with initial conditions given on the interval $[-\tau,0]$. Setting the initial conditions to zero yields the following system of linear differential equations

$$\frac{\mathrm{d}mRNA(t)}{\mathrm{d}t}=f_0-\delta\ mRNA(t), \tag{C 1}$$

$$\frac{\mathrm{d}Hes1(t)}{\mathrm{d}t}=\beta\ mRNA(t)-\alpha\ Hes1(t), \tag{C 2}$$

with the solutions

$$mRNA(t)=\frac{f_0}{\delta}\left(1-e^{-\delta t}\right), \tag{C 3}$$

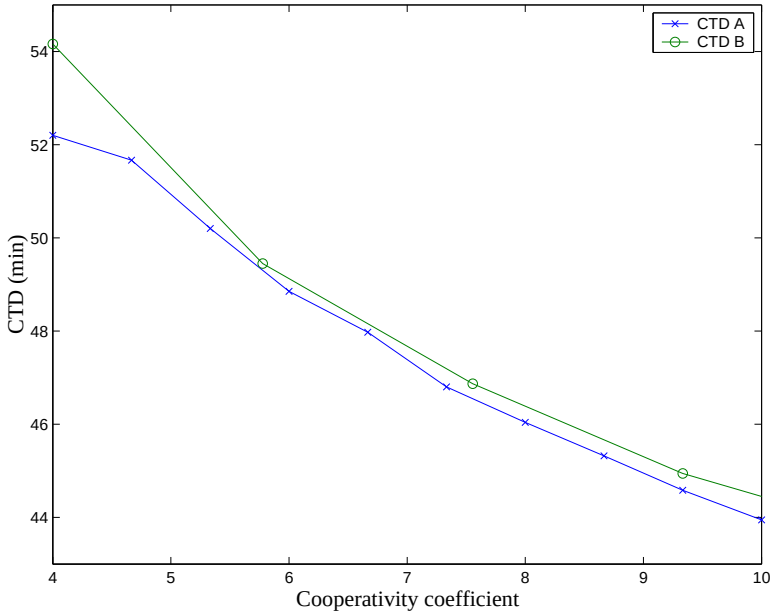

Figure 7. Characteristic turnaround durations for Models A and B (*solid lines with circles and x*). For plotting these curves, a period of 120 min was assumed. That is, for a given h, τ was determined to give a period of 120 min (*dashed lines with circles and x*).

$$Hes1(t) = \frac{\beta f_0}{\alpha\delta}\left(1 + \frac{\delta e^{-\alpha t} - \alpha e^{-\delta t}}{\alpha - \delta}\right). \tag{C 4}$$

These solutions are exact for $0 \leq t \leq \tau$ for zero initial conditions. The solution for *Hes1* is a not a convenient expression, but by letting $\alpha \to \delta$, and evaluating at $t = \tau$ we have

$$Hes1(\tau) = \frac{\beta f_0}{\delta^2}\left(1 - e^{-\delta\tau}(1 + \tau\delta)\right). \tag{C 5}$$

The term in parenthesis is a constant of the order of 1. Because estimated values for τ are of the same order as the Hes1 protein and mRNA half-lives, we take the delay τ to be equal to the mRNA half-life, $\tau = \ln 2/\delta$, and we obtain

$$Hes1(\tau) = \frac{\beta f_0}{2\delta^2}(1 - \ln 2). \tag{C 6}$$

If we assume that the steady-state Hes1 level is $Hes1_* = \beta/\alpha = \beta/\delta$, the ratio between $Hes1(\tau)$ and the steady-state Hes1 level can be computed as given in equation (3.5).

References

Bessho, Y. & Kageyama, R., 2003 Oscillations, clocks and segmentation. *Curr. Opin. Genet. Dev.* **13**, 379–384.

Beuter, A., Glass, L., Mackey, M. C. & Titcombe, M. S., eds., 2003 *Nonlinear Dynamics in Physiology and Medicine*, vol. 25 of *Interdisciplinary Applied Mathematics*. New York: Springer-Verlag.

Bolouri, H. & Davidson, E. H., 2003 Transcriptional regulatory cascades in development: Initial rates, not steady state, determine network kinetics. *Proc. Natl. Acad. Sci. USA* **100**, 9371–9376.

Christ, B. & Ordahl, C. P., 1995 Early stage of chick somite development. *Anat. Embryo. (Berl.)* **191**, 381–396.

Engelborghs, K., Luzyanina, T. & Samaey, G., 2001 DDE-BIFTOOL v. 2.00: a matlab package for bifurcation analysis of delay differential equations. Katholieke Universiteit Leuven, http://www.cs.kuleuven.ac.be/ koen/.

Ferrell, J. E. J., 1996 Tripping the switch fantastic: How a protein kinase can convert graded inputs into switch-like outputs. *TIBS* **21**, 460–466.

Gao, X., Chandra, T., Gratton, M. O., Quelo, I., Prud'homme, J., Stifani, S. & St-Arnaud, R., 2001 Hes6 acts as a transcriptional repressor in myoblasts and can induce the myogenic differentiation program. *J. Cell Biol.* **154**, 1161–1171.

Ghaemmaghami, S., Huh, W.-K., Bower, K., Howson, R. W., Belle, A., Dephoure, N., O'Shea, E. K. & Weissman, J. S., 2003 Global analysis of protein expression in yeast. *Nature* **425**, 737–741.

Goodwin, B. C., 1965 Oscillatory behavior in enzymatic control processes. *Adv. Enzyme Regul.* **3**, 425–438.

Gossler, A. & Hrabe de Angelis, M., 1998 Somitogenesis. *Curr. Top. Dev. Biol.* **38**, 225–287.

Griffith, J. S., 1968 Mathematics of cellular control processes. I. Negative feedback to one gene. *J. Theor. Biol.* **20**, 202–208.

Hale, J. K. & Verduyn-Lunel, S. M., 1993 *Introduction to Functional Differential Equations*, vol. 99 of *Applied Mathematical Sciences*. New York: Springer-Verlag.

Heitzler, P. & Simpson, P., 1991 The choice of cell fate in the epidermis of drosophila. *Cell* **64**, 1083–1092.

Hirata, H., Yoshiura, S., Ohtsuka, T., Bessho, Y., Harada, T., Yoshikawa, K. & Kageyama, R., 2002 Oscillatory expression of the bHLH factor Hes1 regulated by a negative feedback loop. *Science* **298**, 840–843.

Hoffmann, A., Levchenko, A., Scott, M. L. & Baltimore, D., 2002 The Ikappa B-NF-kappa B signaling module: Temporal control and selective gene activation. *Science* **298**, 1241–1245.

Ishibashi, M., Ang, S. L., Shiota, K., Nakanishi, S., Kageyama, R. & Guillemot, F., 1995 Targeted disruption of mammalian hairy and enhancer of split homolog-1 (hes-1) leads to up-regulation of neural helix-loop-helix factors, premature neurogenesis, and severe neural tube defects. *Genes Dev.* **24**, 3136–3148.

Jensen, M. H., Sneppen, K. & Tiana, G., 2003 Sustained oscillations and time delays in gene expression of protein Hes1. *FEBS Lett.* **541**, 176–177.

Jimenez, G., Paroush, Z. & Ish-Horowicz, D., 1997 Groucho acts as a corepressor for a subset of negative regulators, including hairy and engrailed. *Genes Dev.* **15**, 3072–3082.

Jouve, C., Palmeirim, I., D., H., Beckers, J., Gossler, A., Ish-Horowicz, D. & Pourqi, O., 2000 Notch signalling is required for cyclic expression of the hairy-like gene hes1 in the presomitic mesoderm. *Development* **127**, 1421–1429.

Lahav, G., Rosenfeld, N., Sigal, A., Geva-Zatorsky, N., Levine, A. J., Elowitz, M. B. & Alon, U., 2004 Dynamics of the p53-Mdm2 feedback loop in individual cells. *Nat. Genet.* **36**, 147–150.

Lev Bar-Or, R., Maya, R., Segel, L. A., Alon, U., Levine, A. J. & Oren, M., 2000 Generation of oscillations by the p53-Mdm2 feedback loop: A theoretical and experimental study. *Proc. Natl. Acad. Sci. USA* **97**, 11 250–11 255.

Lewis, J., 2003 Autoinhibition with transcriptional delay: A simple mechanism for the zebrafish somitogenesis oscillator. *Curr. Biol.* **13**, 1398–1408.

McLarren, K. W., Thériault, F. M. & Stifani, S., 2001 Association with the nuclear matrix and interaction with Groucho and RUNX proteins regulate the transcription repression activity of the basic helix loop helix factor Hes1. *J. Biol. Chem.* **276**, 1578–1584.

Monk, N. A. M., 2003 Oscillatory expression of Hes1, p53, and NF-κB driven by transcriptional time delays. *Curr. Biol.* **13**, 1409–1413.

Murray, J. D., 1993 *Mathematical Biology*, vol. 19 of *Biomathematics Texts*. 2nd edn. Berlin: Springer-Verlag.

Nuthall, H. N., Husain, J., McLarren, K. W. & Stifani, S., 2002 Role for Hes1-induced phosphorylation in groucho-mediated transcriptional repression. *Mol. Cell Biol.* **22**, 389–399.

Ohsako, S., Hyer, J., Panganiban, G., Oliver, I. & Caudy, M., 1994 Hairy function as a dna-binding helix-loop-helix repressor of drosophila sensory organ formation. *Genes Dev.* **8**, 2743–2755.

Proush, Z., Finley, R. L. J., Kidd, T., Wainwright, S. M., Ingham, P. W., Brent, R. & Ish-Horowicz, D., 1994 Groucho is required for drosophila neurogenesis, segmentation, and sex determination and interacts directly with hairy-related bhlh proteins. *Cell* **79**, 805–815.

Santillan, M. & Mackey, M. C., 2004*a* Influence of catabolic repression and inducer exclusion on the bistable behavior of the lac operon. *Biophys. J.* **86**, 1282–1292.

Santillan, M. & Mackey, M. C., 2004*b* Why the lysogenic state of λ phage is so stable: a mathematical modelling approach. *Biophys. J.* **86**, 75–84.

Schnell, S. & Maini, P., 2000 Clock and induction model for somitogenesis. *Devel. Dynam.* **217**, 415–420.

Strogatz, S. H., 1994 *Nonlinear Dynamics and Chaos: With applications to physics, biology, chemistry, and engineering*. Studies in Nonlinearity. Reading, MA: Perseus Books.

Takebayashi, K., Sasai, Y., Sakai, Y., Watanabe, T., Nakanishi, S. & Kageyama, R., 1994 Structure, chromosomal locus, and promoter analysis of the gene encoding the mouse helix-loop-helix factor HES-1. Negative autoregulation through the multiple N box elements. *J. Biol. Chem.* **269**, 5150–5156.

Tyson, J. J. & Othmer, H. G., 1978 The dynamics of feedback control circuits in biochemical pathways. *Prog. Theor. Biol.* **5**, 1–62.